ТЕОРЕТИЧЕСКИЕ ОСНОВЫ ХИМИЧЕСКОЙ ТЕХНОЛОГИИ

THEORETICAL BASES OF CHEMICAL TECHNOLOGY

ISSN 2410-6593 (Print), ISSN 2686-7575 (Online)

https://doi.org/10.32362/2410-6593-2021-16-2-113-124

УДК 548.737

RESEARCH ARTICLE

Structural characterization of hydrogen bonding for antipyrine derivatives: Single-crystal X-ray diffraction and theoretical studies

Nataliya S. Rukk[1,@], Ravshan S. Shamsiev[1], Dmitry V. Albov[2], Svetlana N. Mudretsova[2]

[1]MIREA – Russian Technological University (M.V. Lomonosov Institute of Fine Chemical Technologies), Moscow, 119571 Russia

[2]Faculty of Chemistry, Lomonosov Moscow State University, Leninskie Gory, Moscow, 119992 Russia

[@]Corresponding author, e-mail: roukkn@inbox.ru

Abstract

Objectives. *The paper is devoted to the crystal structure characterization of 5-methyl-2-phenyl-4H-pyrazol-3-one (compound **I**) and 2-(4-chlorophenyl)-5-methyl-4H-pyrazol-3-one (compound **II**).*

Methods. *Single-crystal X-ray diffraction studies and theoretical calculations: Density functional theory and quantum theory of atoms in molecules.*

Results. *In the solid state, the crystal structure of compound **I** is characterized by the alternation of OH and NH tautomers connected via O–H---O and N–H---N hydrogen bonds. For compound **II**, the existence of chains built from the NH monomers via hydrogen bonding can be explained by the peculiarities of cooperative effects. In the framework of quantum theory of atoms in molecules, the following topological characteristics are calculated for all dimers: electron density, Laplacian of electron density, density of kinetic, potential, and total energy in the critical point of the intermolecular hydrogen bond. It is concluded that the hydrogen bond in dimers **1**–**4**, **7** (compound **I**), and **8**–**11** (compound **II**) can be assigned to the intermediate (between covalent and dispersion types) interaction owing to hydrogen bond formation with the participation of electronegative oxygen- (and/or nitrogen-) atoms, whereas H-bond in dimers **5** and **6** (compound **I**) can be attributed to the dispersion one (no hydrogen bond formation or weak H-bond formation), and it represents the weak interaction, being in agreement with length for intermolecular hydrogen bond in dimers. The electron density and total energy density values demonstrate that the strongest intermolecular H-bonds take place in dimers **1** (OH---O), **4** (OH---O), **7** (OH---N), **8** (OH---O), **9** (NH---N), and **11** (OH---N). The results obtained for compounds **I** and **II** are compared with data for antipyrine (1,2-dihydro-1,5-dimethyl-2-phenyl-3H-pyrazol-3-one; compound **III**).*

Conclusions. *An important role of intermolecular hydrogen bonding in the crystal packing, molecule association and self-organization via dimer- or more extended species formation has been demonstrated.*

Keywords: *antipyrine and its derivatives, 5-methyl-2-phenyl-4H-pyrazol-3-one, 2-(4-chlorophenyl)-5-methyl-4H-pyrazol-3-one, tautomers, hydrogen bonding, density functional theory (DFT) and quantum theory of atoms in molecules (QTAIM) calculations, crystal structure*

For citation: Rukk N.S., Shamsiev R.S., Albov D.V., Mudretsova S.N. Structural characterization of hydrogen bonding for antipyrine derivatives: Single-crystal X-ray diffraction and theoretical studies. *Tonk. Khim. Tekhnol. = Fine Chem. Technol.* 2021;16(2):113–124. https://doi.org/10.32362/2410-6593-2021-16-2-113-124

НАУЧНАЯ СТАТЬЯ

Структурное описание водородной связи в производных антипирина: рентгеноструктурные и теоретические исследования

Н.С. Рукк[1,@], Р.С. Шамсиев[1], Д.В. Альбов[2], С.Н. Мудрецова[2]

[1]МИРЭА – Российский технологический университет (Институт тонких химических технологий им. М.В. Ломоносова), Москва, 119571 Россия
[2]Московский государственный университет им. М.В. Ломоносова, химический факультет, Москва, 119962 Россия
[@]Автор для переписки, e-mail: roukkn@inbox.ru

Аннотация

Цели. *Работа посвящена рассмотрению особенностей кристаллического строения для 5-метил-2-фенил-4H-пиразол-3-она,* ***I****, и 2-(4-хлорфенил)-5-метил-4H-пиразол-3-она,* ***II****, в сравнении с результатами теоретических расчетов.*
Методы. *Рентгеноструктурный анализ и расчеты в рамках теории функционала плотности и квантовой теории атомов в молекулах.*
Результаты. *Показано, что кристаллическая структура* ***I*** *в твердом агрегатном состоянии характеризуется альтернацией OH и NH таутомеров, связанных посредством водородных связей O–H---O и N–H---N. Для соединения* ***II*** *существование цепочек из связанных водородной связью мономеров NH объясняется особенностями кооперативных эффектов и с теоретической точки зрения. В рамках квантовой теории атомов в молекулах (QTAIM) для всех димеров в критической точке межмолекулярной водородной связи были рассчитаны топологические параметры: электронная плотность, лапласиан электронной плотности, плотность кинетической, потенциальной и полной энергии. Показано, что водородная связь в димерах* ***1–4****,* ***7*** *(соединение* ***I****) и* ***8–11*** *(соединение* ***II****) относится к взаимодействию промежуточного типа (между ковалентным и дисперсионным взаимодействием) за счет образования водородных связей с участием электроотрицательных атомов кислорода (и/или атомов азота), а водородная связь в димерах* ***5*** *и* ***6*** *(соединение* ***I****) – к дисперсионному типу (отсутствие водородной связи или образование слабой H-связи) и представляет собой слабое взаимодействие, что коррелирует с длиной межмолекулярной водородной связи в димерах. На основании анализа значений электронной плотности и плотности полной энергии показано, что наиболее сильные межмолекулярные H-связи реализуются в димерах* ***1*** *(OH---O),* ***4*** *(OH---O),* ***7*** *(OH---N),* ***8*** *(OH---O),* ***9*** *(NH---N) and* ***11*** *(OH---N). Результаты, полученные для* ***I*** *и* ***II****, сопоставлены с данными для 1,2-дигидро-1,5-диметил-2-фенил-3H-пиразол-3-она,* ***III****.*
Выводы. *Показана важная роль межмолекулярной водородной связи в кристаллической упаковке, ассоциации и самоорганизации молекул.*

Ключевые слова: *антипирин и его производные, 5-метил-2-фенил-4H-пиразол-3-он, 2-(4-хлорфенил)-5-метил-4H-пиразол-3-он, таутомеры, водородная связь, теория функционала плотности, квантовая теория атомов в молекулах, кристаллическая структура*

Для цитирования: Рукк Н.С., Шамсиев Р.С., Альбов Д.В., Мудрецова С.Н. Структурное описание водородной связи в производных антипирина: рентгеноструктурные и теоретические исследования. *Тонкие химические технологии.* 2021;16(2):113–124 (Eng.). https://doi.org/10.32362/2410-6593-2021-16-2-113-124

INTRODUCTION

Antipyrine (1,2-dihydro-1,5-dimethyl-2-phenyl-3*H*-pyrazol-3-one; compound **III**) and related compounds are known to possess a number of bioactive properties, such as analgesic and antipyretic ones. They form a large number of complexes with alkaline-, transition-, and rare-earth metals [1–8]. From this point of view, searching for new ligands (including representatives of antipyrine-based ones) is very important [4, 9]. Using the method of computer prognosis based on the Prediction of Activity Spectra for Substances (PASS) system [10], it has been demonstrated that some pyrazolone derivatives, such as 5-methyl-2-phenyl-4*H*-pyrazol-3-one (compound **I**) and 2-(4-chlorophenyl)-5-methyl-4*H*-pyrazol-3-one (compound **II**), possess a relatively high probability of antimetastatic activity. It should be underlined that the compound properties are determined mainly by the specific features of chemical bonding, including hydrogen bonding and intermolecular interactions, between structural units. These distinguishing features are responsible for the self-organization of ions and molecules in crystal packing with the formation of channels opened to the intercalation of small species, for example, complexes with neridronic acid (6-amino-1-hydroxyhexylidene-1,1-bisphosphonic acid) showing promise for treating osteogenesis and the Paget's disease [11]. In the case of solvation (e.g., styryl dyes of the benzoselenazole series), the system of hydrogen bonding makes the structure more rigid compared with the non-solvation one owing to the solvate molecules participation in the hydrogen bond formation [12]. This results in different photocycloaddition reactivity of the solvated and non-solvated compounds and thus a decreased reaction rate for the solvated species. The same has been demonstrated [13] for water molecules and imidazolium salts with respect to the interaction and formation of guest(H_2O)@host (ionic liquid [IL]) complexes through strong H-bonds involving the hydrogen atoms of water molecules and nitrogen atoms of IL anions to produce a quest@host supramolecular structure. Many biologically active molecules contain multiple hydrogen-bonding sites; e.g., barbiturates, a class of compounds widely used for their physiological action as sedatives and anticonvulsants, contain both donor and acceptor atoms for multiple hydrogen-bonding formation. It should be underlined that crystal engineering and design allow obtaining different solid state structures in cocrystals of barbiturate and melamine molecules (linear tape, crinkled tape, or cyclic hexamer) [14]. The hydrogen-bonding importance and its impact on drug efficacy have been demonstrated [15]. In this connection the aim of this paper is to explain structural particularities and their comparison with results of theoretical studies for compounds **I**, **II**, and **III**.

EXPERIMENTAL

Compounds **I**, **II** (*Sigma-Aldrich*, St. Louis, Missouri, USA), and **III** (All-Russian Product Classifier 931335, chem. pure) were first recrystallized from ethanol. Single crystals were grown from saturated aqueous solutions by isothermal evaporation of the solvent at ambient temperature (ca. 20 °C). Thermogravimetric and differential scanning calorimetric (STA-409 Differential Scanning Calorimeter, *Netzsch*, Germany) measurements were carried out over the temperature range 293–573 K with a heating rate of 10 K/min under a helium atmosphere. Aluminum oxide was used as a reference material.

Computational methods

The tautomers of compounds **I** and **II** (Scheme 1) were examined by density functional theory using the Priroda package [16]. Calculations were made using the Perdew–Burke–Ernzerhof (PBE) exchange-correlation functional [17] and TZ2P Gaussian-type basis sets. The solvation effects were estimated in Gaussian 09 [18] using the polarizable continuum model and solvation model based on density (PCM–SMD; water used as solvent, ε = 78.3553). Vibrational harmonic frequency analysis was conducted for the optimized geometries to ensure that a true local minimum was present with no imaginary frequencies. The starting atomic coordinates of compounds were taken from the X-ray refinement results. Convergence criteria for self-consistent field

cycles and geometry optimization were 1×10^{-6} and 1×10^{-5} a.u., respectively. The quantum-topological characteristics of electron density in the critical points of the intermolecular hydrogen bond were calculated in the framework of the quantum theory of atoms in molecules (QTAIM) using the Multiwfn 3.6 program [19].

Single-crystal X-ray crystallography

Crystallographic data were collected and refined on CAD-4 EXPRESS diffractometer[1]. Data reduction was carried out using XCAD4[2]. The following programs were used for theoretical modeling: SHELXS97 for structure solving [20], SHELXL97 for structure refining [20], and Mercury for molecular graphics [21]. The results are given in Table A1 (see Appendix A, pages 125–126).

CCDC 1891632-1891634 contain the supplementary crystallographic data for this paper. These data can be obtained free of charge from The Cambridge Crystallographic Data Centre via http://www.ccdc.cam.ac.uk.

RESULTS AND DISCUSSION

There are three possible tautomers for compounds **I** and **II** (CH: **Ia**, **IIa**; NH: **Ib**, **IIb**; OH: **Ic**, **IIc**; Scheme 1, Table 1) [22]. Here we compare theoretical and single-crystal X-ray diffraction data to examine the crystal packing particularities of compounds **I**–**III**. The following order of stability for compound-**I** tautomers in the gas phase was derived from Table 1: **Ia** (CH) > **Ib** (NH) > **Ic** (OH) [22]. The same order of relative stability was theoretically obtained, the results of which are shown in Table 2. Calculation results of Gibbs free energy (ΔG_{298}) values considering solvation effects demonstrate a slightly lower energy gap between **Ia** and **Ib** and a slightly higher energy gap between **Ib** and **Ic** (0.0, 24.4, and 31.2 vs. 0.0, 9.1, and 28.4 kJ·mol^{-1}, respectively, Table 2). The same tendency can be observed for compound **II** (Table 2).

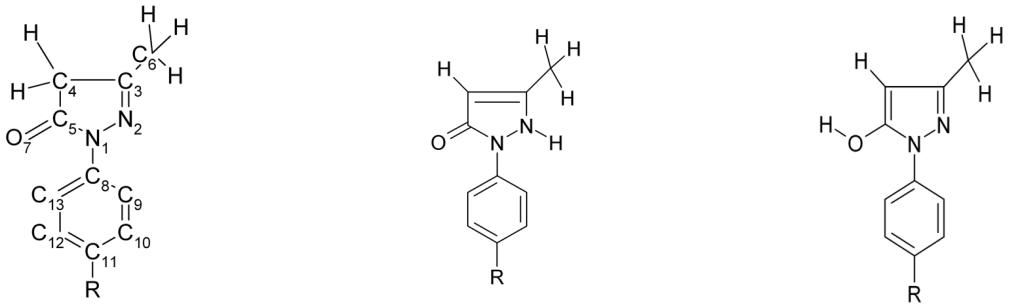

CH **Ia, IIa** | **NH** **Ib, IIb** | **OH** **Ic, IIc**

Scheme 1. Different possible tautomers for compounds **I** and **II**: R = H for the former and R = Cl for the latter.

Table 1. Calculated torsion angles (ω, °), heat of formation (ΔH_f), relative energies (ΔE), and dipole moments (μ) of the tautomers for compound **I** [22]

Method	Tautomer	ω, ° [C(O)–N_1–C_8–C_9]	ω,° [H–N_2–N_1–C_8]	ΔH_f (kJ·mol^{-1}) or ΔE (kJ·mol^{-1})	μ, Debye
AM1	**Ia (CH)**	155.6	–	0.0	2.68
	Ib (NH)	−130.9	88.9	51.51	3.99
	Ic (OH)	−142.6	–	52.80	2.06
PM3	**Ia (CH)**	124.3	–	0.0	2.46
	Ib (NH)	−98.3	86.7	18.58	3.73
	Ic (OH)	−130.7	–	34.14	2.53
HF/6-31G*	**Ia (CH)**	166.9	–	0.0	3.64
	Ib (NH)	−134.9	73.0	36.02	5.25
	Ic (OH)	−132.0	–	52.01	2.31
B3LYP/6-31G*	**Ia (CH)**	177.7	–	0.0	3.31
	Ib (NH)	−149.5	63.0	32.76	5.03
	Ic (OH)	−140.6	–	43.97	2.09

[1] Enraf_Nonius CAD_4 Software. Version 5.0. Delft (The Netherlands): Enraf_Nonius, 1989.
[2] Harms K., Wokadlo S. XCAD4. University of Hamburg, Germany.

Table 2. Calculated torsion angles (ω, °), relative energies (ΔE), Gibbs free energy (ΔG_{298}), Gibbs free energy with PCM–SMD corrections ($\Delta G_{298,solv}$), and dipole moments (μ) for the tautomers of compounds **I**, **II**, and **III**

PBE/3z	ω, °	ω, °	ΔE	ΔG_{298}	$\Delta G_{298,solv}$	μ
	$C(O)–N_1–C_8–C_9$	$H–N_2–N_1–C_8$	kJ·mol^{-1}			Debye
Ia	179.7	–	0.0	0.0	0.0	3.39
Ib	−149.5	61.8	19.3	24.4	9.1	5.15
Ic	−154.6	–	26.2	31.2	28.4	2.68
IIa	179.8	–	0.0	0.0	0.0	5.11
IIb	−148.5	63.7	20.2	25.2	8.5	6.02
IIc	−156.5	–	26.5	31.4	28.4	4.19
III	−127.7	–	–	–	–	5.36

We calculated the parameters of dimer formation from the monomers of compounds **I** and **II**, and compared the experimental and theoretical results (Table 3). The crystal structure of compound **I** is characterized by the alternation of **Ib** and **Ic** tautomers (Fig. 1a and b) connected via the O–H---O=C and N–H---N hydrogen bonds ($r_{O-H---O}$ = 2.479 Å, $r_{N–H---N}$ = 2.800 Å, Table 3, entries **1** and **2**). Extended infinite chains can be observed (Fig. 1b), as confirmed by the calculation results (Table 3, entries **1**–**7**). For the stronger O–H---O H-bonding between the **Ib** and **Ic** tautomers (r_{O---HO} = 2.62 Å, $r_{N–H---N}$ = 2.98 Å, Table 3, entries **1** and **2**) the **Ib** and **Ic** self-organization in the solid state possibly begins with the formation of the stronger O–H---O H-bonding, followed by the formation of N–H---N one. This can explain the absence of the **Ib**–**Ib** (N–H---O), **Ia**–**Ic** (O---H–O), **Ic**–**Ic** (N---H–O), and **Ia**–**Ia**, **Ia**–**Ib** (N---H–N) dimers in the solid state (Table 3, entries **3**, **4**, **7** and **5**, **6**), as confirmed by the ΔG_{298} values for the tautomer dimerization (Table 3, entries **1**–**7**, column 6).

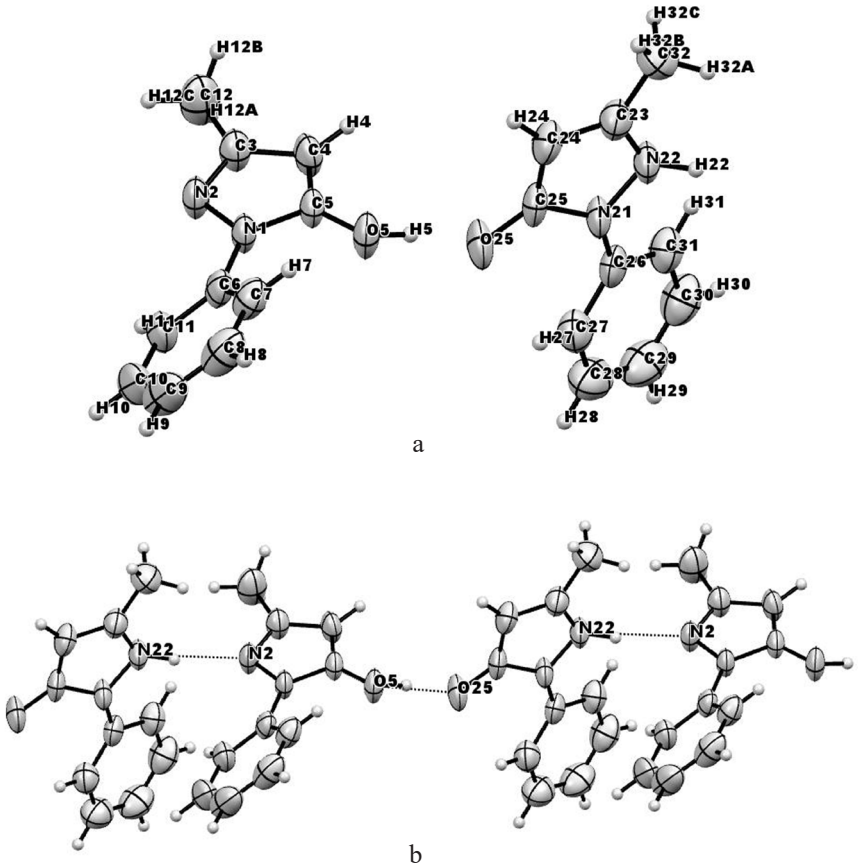

Fig. 1. Asymmetric unit of compound **I** with the crystallographic numbering scheme. Displacement ellipsoids are drawn at the 50% probability level, (a); H-bonding between **OH**- and **NH**-tautomers (b).

Compound **II** exists as the NH tautomer (Fig. 2), the molecules of which are linked by N–H---O-type H-bonds ($r_{N-H---O}$ = 2.729 Å; Fig. 2a and Table 3, entry **10**). This results in the formation of non-interacting extended chains with mutual anti-orientation (Fig. 2b). In the crystalline state, compound **II** consists of **IIb** tautomers, not **IIa** tautomers. The calculated ΔG_{298} values for **IIb** and **IIc** dimerization (**IIa** unable to form dimers with strong hydrogen bonding) demonstrate that the **IIb**–**IIc** (O-H---O) dimer is the most stable (ΔG_{298} = −13.3 kJ·mol^{-1}), followed by the **IIb**–**IIb** (N-H---O) dimer (ΔG_{298} = −3.7 kJ·mol^{-1}; Table 3, entries **8** and **10**). It is easy to imagine that the elongation of the chain built from the **IIb** monomers due to H-bonding (Fig. 2) results in energy gain growth with the number of monomers due to the predominance of the enthalpy contribution (ΔH_{298} = −39.2 kJ·mol^{-1}) over the entropy one ($-T\Delta S_{298}$ = 35.5 kJ·mol^{-1}; Table 3, entry **10**). The formation of chains built from the **Ib** tautomers is possible, but, in this case, the enthalpy contribution is approximately equal to the entropy contribution (Table 3, entry **3**), which can explain the differing mode of monomer alteration for compound **I** (**Ib**–**Ic** [O---H-O] dimer existence).

For all dimers **1**–**11**, the following topology characteristics were calculated using QTAIM theory: electron density (ρ), Laplacian of electron density ($\nabla^2\rho$), density of kinetic (*G*), potential (*V*), and total energy (*H*) in the critical point of the intermolecular hydrogen bond (Table 4). On the basis of the $\nabla^2\rho$ and *H* signs as well as the *V*/*G* (1 < |*V*|/*G* < 2) ratio, it can be concluded that hydrogen bond in dimers **1**–**4** and **7**–**11** can be assigned to the intermediate (between covalent and dispersion types) interaction, whereas the H-bond in dimers **5** and **6** can be assigned to the dispersion interaction, i.e., the weak interaction. Analysis of ρ and *H* values demonstrates that the strongest intermolecular H-bonds take place in dimers **1** (O-H---O), **4** (O-H---O), **7** (O-H---N), **8** (O-H---O), **9** (N-H---N), and **11** (O-H---N). The same dimers are characterized by the shortest X-H---Y distances and by a non-significant increase in the electron localization function (η). By comparing these results with the Gibbs free energy values for dimerization, it can be concluded that the dimer interaction energy is not sufficiently strong to overcome entropy loss during their formation. However, in spite of the H-bond-favorable topology characteristics, the formation of dimers **9** and **11** is unlikely due to the positive ΔG_{298} value.

Experimental data for compounds **I**–**III** are given in Appendix A (Tables A1–A10, pages 125–137).

Packing for compound **III** is characterized by the absence of H-bonding and is based on the presumably steric requirements (Fig. 3, Tables A1, A8–A10), the crystallographic parameters of which are consistent with the existing literature [23–25]. The experimental and theoretical results are confirmed by the thermal analysis data. The melting points for the compounds in question are as follows: 397.6–398.4 (**I**), 431.8–436.3 (**II**), and 381.5–381.9 K (**III**), the melting enthalpy being equal to 18.5, 12.3, and ca. 16.7 kJ·mol^{-1} for (**I**), (**II**), and (**III**), respectively. The order of the latter values is possibly due

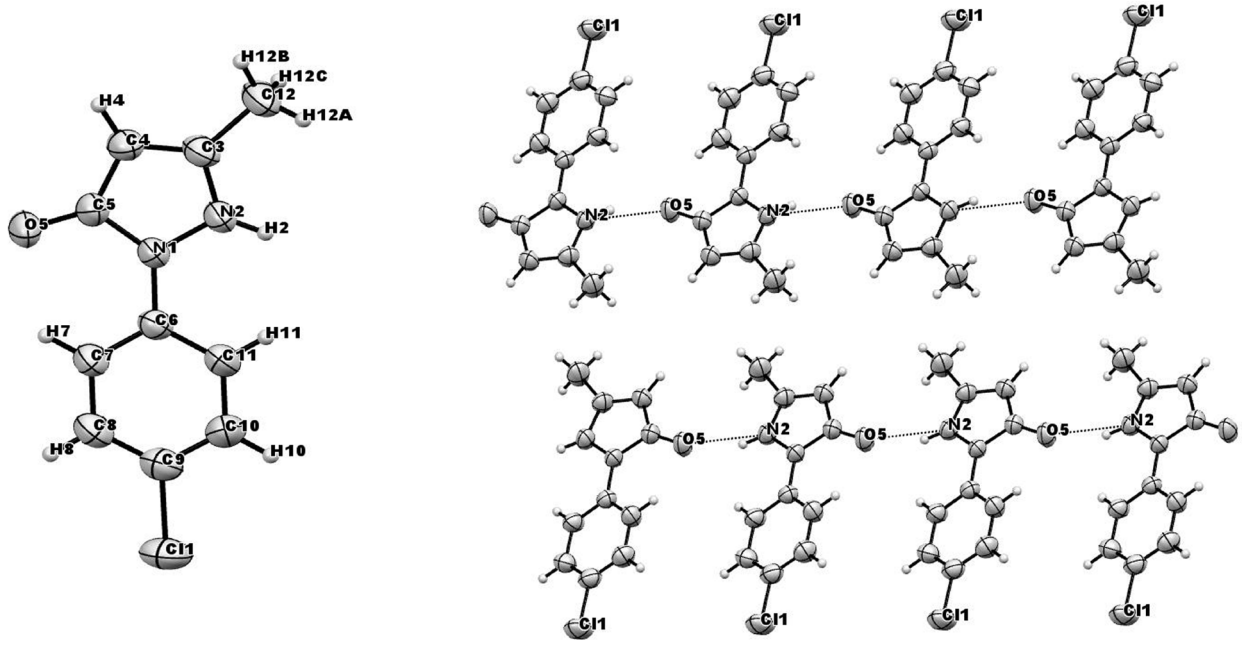

a b

Fig. 2. Asymmetric unit of compound **II** with the crystallographic numbering scheme. Displacement ellipsoids are drawn at the 50% probability level, (a); H-bonding between **NH**-tautomers (b).

Table 3. Description of dimer formation (ΔH_{298} is enthalpy and ΔS_{298} is entropy) from the corresponding monomers of compounds **I** and **II**

Entry	The species label and sketch	H-bond type and length, Å	ΔH_{298}	$-T\Delta S_{298}$	ΔG_{298}
		(calc./exp.)	kJ·mol^{-1}		
1	2	3	4	5	6
1	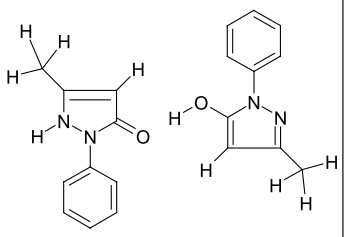 **Ib**–**Ic** dimer (O---HO)	O---H-O 2.62/2.479	−48.4	37.6	−10.8
2	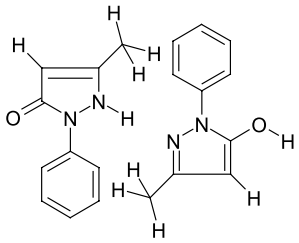 **Ib**–**Ic** dimer (NH---N)	N-H---N 2.98/2.800	−28.8	39.6	10.9
3	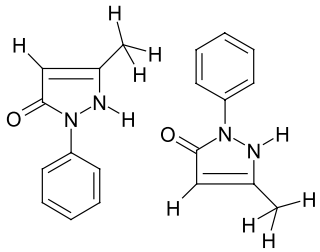 **Ib**–**Ib** dimer (NH---O)	N-H---O 2.81	−38.1	37.6	−0.6
4	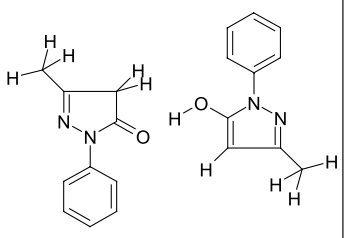 **Ia**–**Ic** dimer (O---HO)	O---H-O 2.65	−41.0	39.9	−1.1

Table 3. Continued

Entry	The species label and sketch	H-bond type and length, Å	ΔH_{298}	$-T\Delta S_{298}$	ΔG_{298}
		(calc./exp.)	kJ·mol^{-1}		
1	2	3	4	5	6
5	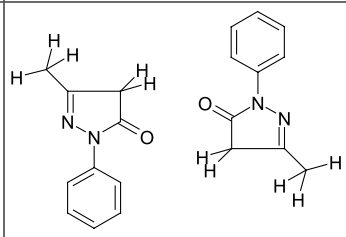 **Ia**–**Ia** dimer	–	−18.8	36.8	18.0
6	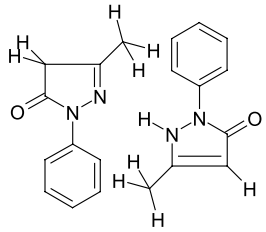 **Ia**–**Ib** dimer (N---HN)	N---H-N 3.08	−20.2	41.8	21.6
7	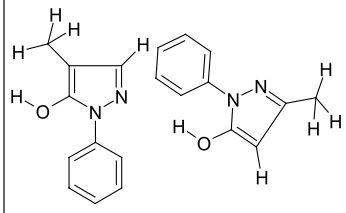 **Ic**–**Ic** dimer (N---HO)	N---H-O 2.70	−33.5	33.5	0.1
8	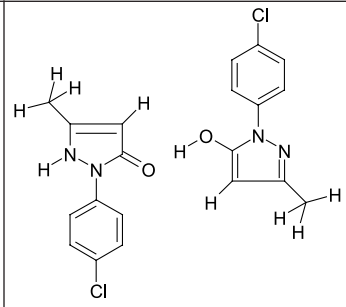 **IIb**–**IIc** dimer (O---HO)	O---H-O 2.62	−48.7	35.5	−13.3
9	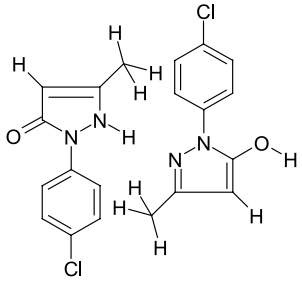 **IIb**–**IIc** dimer (NH---N)	N-H---N 2.97	−28.4	38.6	10.2

Table 3. Continued

Entry	The species label and sketch	H-bond type and length, Å (calc./exp.)	ΔH_{298}	$-T\Delta S_{298}$	ΔG_{298}
			kJ·mol^{-1}		
1	2	3	4	5	6
10	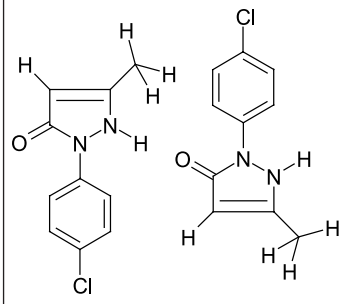 **IIb**–**IIb** dimer (NH---O)	N-H---O 2.81/2.729	−39.2	35.5	−3.7
11	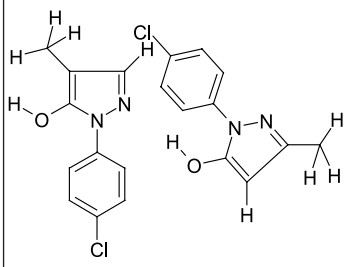 **IIc**–**IIc** dimer (N---HO)	N---H-O 2.70	−36.0	44.5	8.5

Table 4. Topology characteristics and length for the dimer intermolecular hydrogen bond

Dimer	ρ, e·Å^{-3}	$\nabla^2\rho$, e·Å^{-5}	*H*, a.u.	*V*, a.u.	*G*, a.u.	η	R(X-H---Y), Å
Compound **I**							
1	0.0294	0.1165	−0.0147	−0.0585	0.0438	0.2540	1.61
2	0.0155	0.0739	−0.0011	−0.0207	0.0196	0.1660	1.94
3	0.0201	0.1067	−0.0037	−0.0341	0.0304	0.1650	1.77
4	0.0265	0.1139	−0.0112	−0.0508	0.0397	0.2261	1.65
5	0.0070	0.0523	0.0027	−0.0076	0.0103	0.0489	2.23
5*	0.0071	0.0527	0.0027	−0.0077	0.0104	0.0493	2.23
6	0.0108	0.0619	0.0014	−0.0127	0.0141	0.0619	2.09
7	0.0270	0.0845	−0.0126	−0.0464	0.0338	0.3011	1.70
Compound **II**							
8	0.0295	0.1168	−0.0148	−0.0588	0.0440	0.2550	1.61
9	0.0296	0.1169	−0.0148	−0.0588	0.0440	0.2552	1.62
10	0.0200	0.1069	−0.0037	−0.0340	0.0304	0.1637	1.77
11	0.0275	0.0843	−0.0132	−0.0475	0.0343	0.3074	1.69

Note: **5*** is for another position of O atoms.

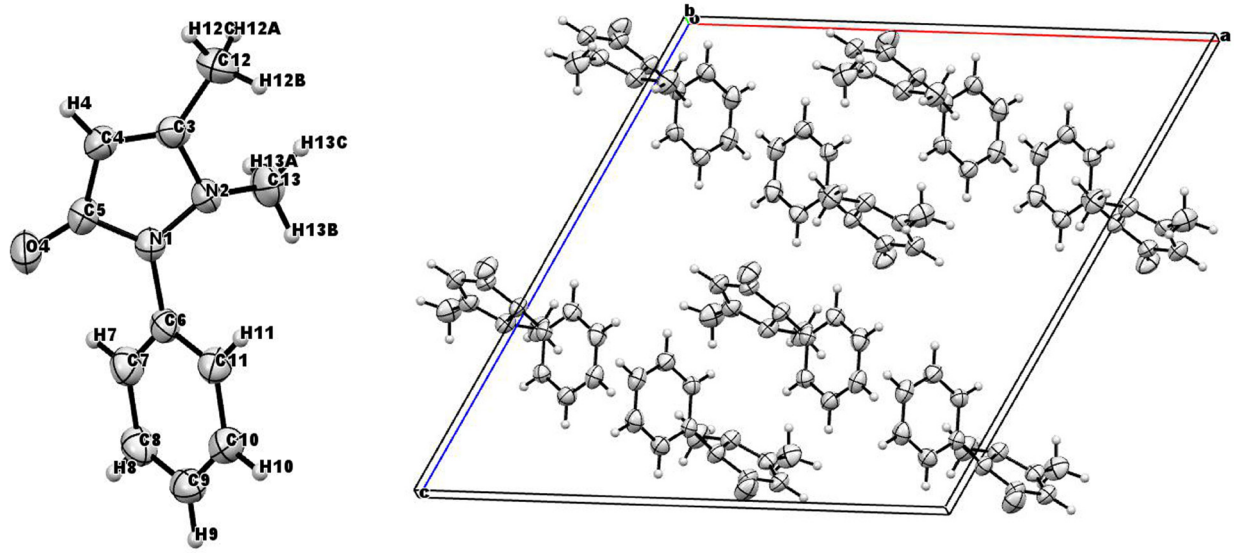

a b

Fig. 3. Asymmetric unit of compound **III** with the crystallographic numbering scheme. Displacement ellipsoids are drawn at the 50% probability level, (a); crystal structure packing (b).

to the absence of hydrogen bonding in compound **III** and the presence of comparatively longer and weaker hydrogen bonds between dimers in compound **II** compared with compound **I**. The wide melting range for compound **II** is possibly related to the intermolecular interactions with participation of chlorine atoms.

CONCLUSIONS

Our study demonstrated that intermolecular hydrogen bonding plays an important role in crystal packing, molecule association, and self-organization, and it explains some contradictions between the theoretical data for the molecules in the gas phase and experimental results for compounds in the solid state. Differentiation was determined between strong interactions due to participation of atoms with high electronegativity (O, N) and the weak (dispersion) ones, the dimer formation being the first step of extended species formation.

APPENDIX A

Supplementary data to this article can be found after this article and online at https://doi.org/10.32362/2410-6593-2021-16-2-113-124 (Supplementary files).

The authors were equally involved in the work on the article.

The authors declare no conflicts of interest.

REFERENCES

1. Vijayan M., Viswamitra M.A. A Refinement of the Structure of Calcium Hexa-antipyrine Perchlorate and a Comparative Study of Some Metal Hexaantipyrine Perchlorates. *Acta Crystallogr.* 1968;B24(8):1067–1076. https://doi.org/10.1107/S0567740868003717

2. Brassy C., Mornon J.-P., Delettre J. Dinitratobis(antipyrine) cobalt(II). *Acta Crystallogr.* 1974;B30(9):2243–2248. https://doi.org/10.1107/S0567740874006832

3. Lenarcik B., Wisniewski M., Gabryszewski M. Complexation capacity of some biologically active derivatives of 5-pyrazolone. *Pol. J. Chem.* 1980;54(10):1869–1874.

4. Maroszová J., Findoráková L., Györyvá K., Koman M., Melník M. Bis(2-chlorobenzoato-κ*O*)bis(phenazone-κ*O*)zinc(II) 0.612-hydrate. *Acta Crystallogr.* 2007;E63(5):m1406–m1407. https://doi.org/10.1107/S1600536807016765

5. Madhu N.T., Radhakrishnan P.K., Grunert M., Weinberger P., Linert F. Antipyrine and its derivatives with first row transition metals. *Rev. Inorg. Chem.* 2003;23(1):1–23. https://doi.org/10.1515/REVIC.2003.23.1.1

6. Rukk N.S., Antsyshkina A.S., Sadikov G.G., Sergienko V.S., Skryabina A.Yu., Osipov R.A., Alikberova L.Yu. Synthesis and Structure of Complex Compounds of Lanthanum, Europium and Scandium Iodides with Antipyrine. *Russ. J. Inorg. Chem.* 2009;54(4):539–542. https://doi.org/10.1134/S0036023609040081

7. Rukk N.S., Albov D.V., Shamsiev R.S., Mudretsova S.N., Davydova G.A., Sadikov G.G., Antsyshkina A.S., Kravchenko V.V., Skryabina A.Yu., Apryshko G.N., Zamalyutin V.V., Mironova E.A. Synthesis, X-ray crystal structure and cytotoxicity studies of lanthanide(III) iodide complexes with anipyrine. *Polyhedron.* 2012;44(1):124–132. https://doi.org/10.1016/j.poly.2012.06.075

8. Rukk N.S., Kuzmina L.G., Albov D.V., Shamsiev R.S., Mudretsova S.N., Davydova G.A., Retivov V.M., Volkov P.V., Kravchenko V.V., Apryshko G.N., Streletskii A.N., Skryabina A.Yu., Mironova E.A., Zamalyutin V.V. Synthesis, X-ray crystal structure and cytotoxicity studies of zinc(II) and cadmium(II) iodide complexes with anipyrine. *Polyhedron.* 2015;102:152–162. https://doi.org/10.1016/j.poly.2015.09.011

9. Li Z.-X., Fei N., Yuan W. Crystal structure of 4-((4-methoxy-benzylidene)-amino)-1,5-dimethyl-2-phenylpyrazolidin-3-ol, $C_{19}H_{19}N_3O_2$. *Z. Kristallogr. NCS.* 2007;222(2):133–134. https://doi.org/10.1524/ncrs.2007.0053

10. Rukk N.S., Skryabina A.Yu., Apryshko G.N. Search for potential antitumor complex compounds of rare earth metals. *Russ. J. Biotherapy.* 2009;8(2):14–15 (in Russ.).

11. Galantsev A.V., Drobot D.V., Dorovatovsky P.V., Khrustalev V.N. Lanthanum Complex with Neridronic Acid: Synthesis and Properties. *Tonk. Khim. Tekhnol. = Fine Chem. Technol.* 2019;14(2):70–77 (in Russ.). https://doi.org/10.32362/2410-6593-2019-14-2-70-77

12. Kuz'mina L.G, Vedernikov A.I., Howard J.A.K., Bezzubov S.I., Alfimov M.V., Gromov S.P. Peculiarities of styryl dyes of the benzoselenazole series crystal packings and their influence on solid phase [2 + 2] photocycloaddition reaction with single crystal retention. *CrystEngComm,* 2016;18:7506–7515. https://doi.org/10.1039/C6CE01426G

13. Zanatta M., Dupont J., Wentz G.N., dos Santos F.P. Intermolecular hydrogen bonds in water@IL supramolecular complexes. *Phys. Chem. Chem. Phys.* 2018;20(17):11608–11614. https://doi.org/10.1039/C8CP00066B

14. Beijer F.H. *Cooperative multiple hydrogen bonding in supramolecular chemistry*. Eindhoven: Technische Universiteit Eindhoven; 1998. 188 p. https://doi.org/10.6100/IR508563

15. Zhai C., Hou B., Peng P., Zhang P., Li L., Chen X. Hydrogen bonding interaction of ascorbic acid with nicotinamide: Experimental and theoretical study. *J. Mol. Liquids.* 2018;249:9–15. https://doi.org/10.1016/j.molliq.2017.11.034

16. Laikov D.N. Fast evaluation of density functional exchange-correlation terms using the expansion of the electron density in auxiliary basis sets. *Chem. Phys. Lett.* 1997;281(1–3):151–156. https://doi.org/10.1016/S0009-2614(97)01206-2

17. Perdew J.P., Burke K., Ernzerhof M. Generalized Gradient Approximation Made Simple. *Phys. Rev. Lett.* 1996;77(18):3865–3868. https://doi.org/10.1103/PhysRevLett.77.3865

18. Gaussian 09, Revision A.02. Frisch M.J., Trucks G.W., Schlegel H.B., Scuseria G.E., Robb M.A., Cheeseman J.R., Scalmani G., Barone V., Petersson G.A., Nakatsuji H., Li X., Caricato M., Marenich A., Bloino J., Janesko B.G., Gomperts R., Mennucci D., Hratchian H.P., Ortiz J.V., Izmaylov A.F., Sonnenberg J.L., Williams-Yang D., Ding F., Lipparini F., Egidi F., Goings J., Peng B., Petrone A., Henderson T., Ranasinghe D., Zakrewski V.G., Gao J., Rega N., Zheng D., Liang W., Hada M., Ehara M., Toyota K., Fukuda R., Hasegawa J., Ishida M., Nakajima T., Honda Y., Kitao O., Nakai H., Vreven T., Throssell K., Montgomery J.A. Jr., Peralta J.E., Ogliaro F., Bearpark M., Heyd J.J., Brothers E., Kudin K.N., Staroverov V.N., Keith T,. Kobayashi R., Normand J., Raghavachari K., Rendell A., Burant J.C., Iyengar S.S., Tomasi J., Cossi M., Millam J.M., Klene M., Adamo C., Cammi R., Ochterski J.W., Martin R.L., Morokuma K., Farkas O., Foresman J.B., Fox D.J., Gaussian, Inc., Wallingford CT, 2016.

19. Lu T., Chen F. Multiwfn: A Multifunctional Wavefunction Analyzer. *J. Comput. Chem.* 2012;33(5):580–592. https://doi.org/10.1002/jcc.22885

20. Sheldrick G.M. Crystal structure refinement with SHELXL. *Acta Crystallogr.* 2015;C71:3–8. https://doi.org/10.1107/S2053229614024218

21. Macrae E.C.F., McCabe P., Pidcock E., Shields G.P. Taylor R., Towler M., van de Streek I. Mercury: visualization and analysis of crystal structures. *J. Appl. Crystallogr.* 2006;39(3):453–457. https://doi.org/10.1107/S002188980600731X

22. Dardonville C., Elguero J., Rozas I., Fernández-Castaño C., Foces-Foces C., Sobrados I. Tautomerism of 1-(2º,4º-dinitrophenyl)-3-methyl-2-pyrazolin-5-one: theoretical calculations, solid and solution NMR studies and X-ray crystallography. *New J. Chem.* 1998;22(12):1421–1430. https://doi.org/10.1039/A805415K

23. Singh T.P., Vijayan M. Structural Studies of Analgesics and Their Interactions. I. The Crystal and Molecular Structure of Antipyrine. *Acta Crystallogr.* 1973;B29:714–720. https://doi.org/10.1107/S0567740873003225

24. Chugunova G.A., Kataeva O.N., Ahlbrecht H., Kurbangalieva A.R., Movchan A.I., Lenstra A.T.H., Geise H.J., Litvinov I.A. Derivatives of 1-phenyl-3-methylpyrazol-2-in-5-thione and their oxygen analogues in the crystalline phase and their tautomeric transformations in solutions and in the gas phase. *J. Mol. Struct.* 2001;570(1–3):215–223. https://doi.org/10.1016/S0022-2860(01)00514-2

25. Wang Q., Zhang Y., Wang R., Yang Y.-L., Zhi F. 5-Methyl-2-phenyl-2H-pyrazol-3-ol. *Acta Crystallogr.* 2008;E64(10):o1924. https://doi.org/10.1107/S1600536808028559

About the authors:

Nataliya S. Rukk, Cand. Sci. (Chem.), Associate Professor, A.N. Reformatskii Department of Inorganic Chemistry, M.V. Lomonosov Institute of Fine Chemical Technologies, MIREA – Russian Technological University (86, Vernadskogo pr., Moscow, 119571, Russia). E-mail: roukkn@inbox.ru. Scopus Author ID 6506769340, Researcher ID I-3151-2016, http://orcid.org/0000-0001-7989-8009

Ravshan S. Shamsiev, Dr. Sci. (Chem.), Professor, Ya.K. Syrkin Department of Physical Chemistry, M.V. Lomonosov Institute of Fine Chemical Technologies, MIREA – Russian Technological University (86, Vernadskogo pr., Moscow, 119571, Russia). E-mail: shamsiev.r@gmail.com. Scopus Author ID 6506076152, Researcher ID L-4526-2016, http://orcid.org/0000-0002-0473-770X

Dmitry V. Albov, Cand. Sci. (Chem.), Senior Scientific Researcher, M.V. Lomonosov Moscow State University (1, Leninskie Gory, Moscow, 119992, Russia). E-mail: dmitryalbov@mail.ru. Scopus Author ID 8375436400.

Svetlana N. Mudretsova, Senior Scientific Researcher, M.V. Lomonosov Moscow State University (1, Leninskie Gory, Moscow, 119992, Russia). Scopus Author ID 6603774709.

Об авторах:

Рукк Наталия Самуиловна, к.х.н., доцент кафедры неорганической химии им. А.Н. Реформатского, Институт тонких химических технологий им. М.В. Ломоносова, ФГБОУ ВО «МИРЭА – Российский технологический университет» (119571, Россия, Москва, пр-т Вернадского, 86). E-mail: roukkn@inbox.ru. Scopus Author ID 6506769340, Researcher ID I-3151-2016, http://orcid.org/0000-0001-7989-8009

Шамсиев Равшан Сабитович, д.х.н., профессор кафедры физической химии им. Я.К. Сыркина, Институт тонких химических технологий им. М.В. Ломоносова, ФГБОУ ВО «МИРЭА – Российский технологический университет» (119571, Россия, Москва, пр-т Вернадского, 86). E-mail: shamsiev.r@gmail.com. Scopus Author ID 6506076152, Researcher ID L-4526-2016, http://orcid.org/0000-0002-0473-770X

Альбов Дмитрий Васильевич, к.х.н., научный сотрудник, МГУ им. М.В. Ломоносова, химический факультет (119992, Россия, Москва, Ленинские Горы, 1). E-mail: dmitryalbov@mail.ru. Scopus Author ID 8375436400.

Мудрецова Светлана Николаевна, старший научный сотрудник, МГУ им. М.В. Ломоносова, химический факультет (119992, Россия, Москва, Ленинские Горы, 1). Scopus Author ID 6603774709.

Поступила: 24.01.2020; получена после доработки: 17.08.2020; принята к опубликованию: 21.04.2021.
The article was submitted: January 24, 2020; approved after reviewing: August 17, 2020; accepted for publication: April 21, 2021.

The text was submitted by the authors in English.

Edited for English language and spelling by Enago, an editing brand of Crimson Interactive Inc.

APPENDIX A

Supplementary data to the research article: Rukk N.S., Shamsiev R.S., Albov D.V., Mudretsova S.N. Structural characterization of hydrogen bonding for antipyrine derivatives: Single-crystal X-ray diffraction and theoretical studies. *Tonk. Khim. Tekhnol. = Fine Chem. Technol.* 2021;16(2):113–124

Table A1. Crystal data and the details of data collection and refinement for compounds **I**, **II**, and **III**

Compound	I	II	III
Empirical formula	$C_{10}H_{10}N_2O$	$C_{10}H_9ClN_2O$	$C_{11}H_{12}N_2O$
Formula weight	174.20	208.64	188.23
Crystal system, Sp. gr., Z	Monoclinic, $P2_1/c$, 8	Triclinic, P–1, 2	Monoclinic, C2/c, 8
a, *b*, *c*, Å	*a* = 10.331(3) *b* = 11.155(4) *c* = 15.880(5)	*a* = 5.8551(12) *b* = 7.674(3) *c* = 11.348(3)	*a* = 16.892(9) *b* = 7.429(3) *c* = 17.776(8)
α, β, γ, °; V, Å^3	90.00, 95.06(3), 90.00; 1822.9 (10)	106.11(2), 94.669(19), 101.51(2); 475.0(2)	90.00, 116.98(5), 90.00; 1987.9(16)
F(000)	736	216	800
D_x, Mg·m^{-3}	1.269	1.459	1.258
Radiation	Cu Kα radiation, λ = 1.5418 Å, Cell parameters from 25 reflections θ = 33°–35°	Cu Kα radiation, λ = 1.5418 Å, Cell parameters from 25 reflections θ = 30°–33°	Ag Kα radiation, λ = 0.56087 Å, Cell parameters from 25 reflections θ = 15°–16°
μ, mm^{-1}	0.68	3.28	0.05
Crystal size, mm^3	0.20 × 0.20 × 0.20 Colorless prisms	0.10 × 0.10 × 0.10 Colorless prisms	0.50 × 0.50 × 0.50 Colorless prisms
Data collection: Enraf Nonius CAD4 diffractometer[3]; radiation source: fine-focus sealed tube; monochromator: graphite; non–profiled ω scans.			
3450 measured reflections, 3450 independent reflections, 2988 reflections with $I > 2\sigma(I)$; R_{int} = 0.0000; θ_{max} = 69.9°, θ_{min} = 4.3°; $h = -12 \rightarrow 12$; $k = 0 \rightarrow 13$; $l = 0 \rightarrow 19$; 1 standard reflection every 120 min; intensity decay: 1%	1952 measured reflections, 1952 independent reflections, 1740 reflections with $I > 2\sigma(I)$; R_{int} = 0.0000; θ_{max} = 74.8°, θ_{min} = 4.1°; $h = -7 \rightarrow 7$; $k = -9 \rightarrow 9$; $l = 0 \rightarrow 14$; 2 standard reflections every 120 min; intensity decay: 2%	9715 measured reflections, 4882 independent reflections, 2820 reflections with $I > 2\sigma(I)$; R_{int} = 0.070; θ_{max} = 28.0°, θ_{min} = 2.0°; $h = -28 \rightarrow 28$; $k = -12 \rightarrow 12$; $l = -29 \rightarrow 15$; 1 standard reflection every 60 min; intensity decay: 2%	

[3] Enraf_Nonius CAD_4 Software. Version 5.0. Delft (The Netherlands): Enraf_Nonius, 1989.

Table A1. Continued

Absorption correction: multiscan [20]. Refinement on F^2. Least-squares matrix: full			
Refinement			
H-atom treatment	H atoms were treated by a mixture of independent and constrained refinement	H-atom parameters constrained	
$R[F^2 > 2\sigma(F^2)]$	0.037	0.057	0.058
w$R(F^2)$	0.102	0.158	0.175
S	1.04	1.06	1.01
Reflections/parameters/ restraints	3450/250/0	1952/128/0	4882/130/0
$\Delta\rho_{max}/\Delta\rho_{min}$, e·Å^{-3}	0.15/−0.11	0.33/−0.22	0.26/−0.30

Note: Z = the number of formula units in the unit cell;
R_{int} = merging error (measure of the precision/reproducibility);
θ_{max} = max θ angle in degrees for the reflection used for measurement of the unit cell;
θ_{min} = min θ angle in degrees for the reflection used for measurement of the unit cell;
Sp. gr. = space group;
μ = absorption coefficient;
λ = wavelength, refers to the radiation used to measure intensities;
V = unit cell volume;
a, *b*, and *c* = cell lengths; α, β, and γ = cell angles;
D_x = calculated density;
I = intensity of reflection;
R = R-factor;
w*R* = weighed R-factor;
F(000) = sum of all electrons in the unit cell;
σ = standard deviation;
S = goodness of fit;
h, *k*, and *l* = Miller indices;
$I > 2\sigma(I)$ = criterion for strong reflections.

Table A2. Fractional atomic coordinates and isotropic or equivalent isotropic displacement parameters (Å^2) for compound **I**

Atom	*x*	*y*	*z*	U_{iso}*/U_{eq}
N1	0.19338 (10)	0.37391 (8)	0.06745 (7)	0.0430 (2)
N2	0.27022 (11)	0.29948 (9)	0.02385 (7)	0.0498 (3)
C3	0.32777 (14)	0.37019 (11)	−0.02844 (9)	0.0518 (3)
C4	0.29077 (14)	0.48962 (11)	−0.01909 (9)	0.0530 (3)
H4	0.3209 (16)	0.5576 (15)	−0.0496 (10)	0.067 (5)*
C5	0.20504 (12)	0.48922 (10)	0.04174 (8)	0.0439 (3)
O5	0.13825 (10)	0.57503 (8)	0.07625 (7)	0.0570 (3)
H5	0.1924 (18)	0.6493 (19)	0.0784 (12)	0.087 (6)*
C6	0.11839 (13)	0.32597 (10)	0.12979 (8)	0.0455 (3)
C7	−0.00259 (14)	0.37340 (13)	0.14200 (9)	0.0555 (3)
H7	−0.0347	0.4389	0.1105	0.067*
C8	−0.07485 (17)	0.32197 (17)	0.20172 (12)	0.0747 (5)
H8	−0.1553	0.3543	0.2110	0.090*
C9	−0.0297 (2)	0.22383 (18)	0.24762 (12)	0.0854 (6)
H9	−0.0802	0.1886	0.2865	0.102*
C10	0.0912 (2)	0.17804 (15)	0.23559 (11)	0.0802 (6)
H10	0.1224	0.1122	0.2670	0.096*
C11	0.16638 (17)	0.22889 (12)	0.17740 (9)	0.0598 (4)
H11	0.2484	0.1984	0.1702	0.072*
C12	0.41644 (18)	0.31848 (16)	−0.08831 (12)	0.0780 (5)
H12A	0.5048	0.3378	−0.0694	0.117*
H12B	0.3954	0.3514	−0.1437	0.117*
H12C	0.4061	0.2330	−0.0904	0.117*
N21	0.30234 (11)	0.96602 (8)	0.07065 (7)	0.0473 (3)
N22	0.26333 (12)	1.04936 (9)	0.00912 (8)	0.0517 (3)
H22	0.2696 (16)	1.1302 (18)	0.0200 (11)	0.075 (5)*
C23	0.16953 (14)	0.99970 (12)	−0.04340 (9)	0.0546 (3)
C24	0.15371 (15)	0.88297 (12)	−0.02102 (10)	0.0564 (4)
H24	0.0945 (16)	0.8289 (15)	−0.0484 (10)	0.068 (5)*
C25	0.23756 (13)	0.85971 (10)	0.05141 (9)	0.0486 (3)
O25	0.26042 (11)	0.76589 (8)	0.09483 (7)	0.0646 (3)
C26	0.41009 (12)	0.98926 (10)	0.12963 (9)	0.0468 (3)
C27	0.42958 (16)	0.92134 (13)	0.20319 (10)	0.0606 (4)

Table A2. Continued

Atom	*x*	*y*	*z*	U_{iso}*/U_{eq}
H27	0.3720	0.8601	0.2137	0.073*
C28	0.53456 (18)	0.94523 (17)	0.26046 (11)	0.0752 (5)
H28	0.5485	0.8987	0.3090	0.090*
C29	0.61888 (18)	1.03716 (19)	0.24653 (13)	0.0799 (5)
H29	0.6887	1.0536	0.2859	0.096*
C30	0.59944 (16)	1.10417 (17)	0.17444 (13)	0.0750 (5)
H30	0.6563	1.1665	0.1652	0.090*
C31	0.49607 (14)	1.08054 (13)	0.11487 (11)	0.0595 (4)
H31	0.4847	1.1256	0.0655	0.071*
C32	0.10490 (19)	1.07208 (16)	−0.11336 (11)	0.0751 (5)
H32A	0.0953	1.1532	−0.0947	0.113*
H32B	0.0208	1.0389	−0.1301	0.113*
H32C	0.1568	1.0710	−0.1606	0.113*

Note: The sign * indicates the isotropic displacement parameters, Å^2.

Table A3. Atomic displacement parameters (Å^2) for compound **I**

Atom	U^{11}	U^{22}	U^{33}	U^{12}	U^{13}	U^{23}
N1	0.0534 (6)	0.0206 (4)	0.0566 (6)	−0.0024 (4)	0.0141 (5)	−0.0016 (4)
N2	0.0611 (7)	0.0248 (5)	0.0661 (7)	0.0017 (4)	0.0207 (5)	−0.0021 (4)
C3	0.0578 (7)	0.0343 (6)	0.0656 (8)	−0.0016 (5)	0.0180 (6)	0.0004 (6)
C4	0.0654 (8)	0.0278 (6)	0.0681 (8)	−0.0062 (6)	0.0182 (7)	0.0068 (6)
C5	0.0535 (7)	0.0206 (5)	0.0582 (7)	−0.0031 (5)	0.0080 (6)	−0.0013 (5)
O5	0.0680 (6)	0.0238 (4)	0.0819 (7)	−0.0005 (4)	0.0224 (5)	−0.0055 (4)
C6	0.0581 (7)	0.0275 (6)	0.0522 (7)	−0.0118 (5)	0.0124 (6)	−0.0068 (5)
C7	0.0565 (8)	0.0460 (7)	0.0652 (8)	−0.0128 (6)	0.0128 (6)	−0.0136 (6)
C8	0.0718 (10)	0.0743 (11)	0.0825 (11)	−0.0306 (9)	0.0328 (9)	−0.0272 (9)
C9	0.1175 (16)	0.0750 (12)	0.0694 (10)	−0.0501(12)	0.0415 (11)	−0.0159 (9)
C10	0.1320 (17)	0.0452 (9)	0.0659 (10)	−0.0267(10)	0.0222 (10)	0.0051 (7)
C11	0.0854 (10)	0.0328 (6)	0.0628 (8)	−0.0065 (6)	0.0152 (7)	0.0018 (6)
C12	0.0865 (12)	0.0592 (10)	0.0951 (12)	0.0037 (8)	0.0462 (10)	−0.0027 (9)
N21	0.0558 (6)	0.0203 (4)	0.0649 (6)	−0.0015 (4)	−0.0003 (5)	−0.0005 (4)
N22	0.0660 (7)	0.0233 (5)	0.0648 (7)	−0.0013 (5)	−0.0004 (6)	−0.0012 (5)
C23	0.0625 (8)	0.0395 (7)	0.0613 (8)	0.0002 (6)	0.0019 (6)	−0.0059 (6)
C24	0.0623 (8)	0.0363 (7)	0.0699 (9)	−0.0102 (6)	0.0020 (7)	−0.0121 (6)

Table A3. Continued

Atom	U^{11}	U^{22}	U^{33}	U^{12}	U^{13}	U^{23}
C25	0.0540 (7)	0.0220 (5)	0.0707 (8)	−0.0033 (5)	0.0099 (6)	−0.0068 (5)
O25	0.0771 (7)	0.0234 (4)	0.0925 (8)	−0.0051 (4)	0.0027 (6)	0.0034 (4)
C26	0.0497 (7)	0.0283 (6)	0.0626 (7)	0.0039 (5)	0.0064 (6)	−0.0092 (5)
C27	0.0675 (9)	0.0459 (8)	0.0683 (9)	0.0036 (7)	0.0058 (7)	0.0002 (7)
C28	0.0793 (11)	0.0766 (11)	0.0676 (10)	0.0117 (9)	−0.0046 (8)	−0.0029 (8)
C29	0.0662 (10)	0.0902 (13)	0.0802 (11)	0.0004 (10)	−0.0099 (9)	−0.0195(10)
C30	0.0607 (9)	0.0674 (10)	0.0966 (13)	−0.0145 (8)	0.0047 (9)	−0.0190(10)
C31	0.0587 (8)	0.0446 (7)	0.0749 (9)	−0.0085 (6)	0.0050 (7)	−0.0059 (7)
C32	0.0907 (12)	0.0627 (10)	0.0691 (10)	0.0040 (9)	−0.0079 (9)	0.0032 (8)

Table A4. Geometric parameters (Å, º) for compound **I**

Atom–Atom	Bond length, Å	Atom–Atom	Bond length, Å
N1–C5	1.3581 (15)	N21–C25	1.3826 (15)
N1–N2	1.3768 (14)	N21–N22	1.3827 (15)
N1–C6	1.4147 (16)	N21–C26	1.4140 (18)
N2–C3	1.3237 (17)	N22–C23	1.3413 (19)
C3–C4	1.3976 (18)	N22–H22	0.92 (2)
C3–C12	1.493 (2)	C23–C24	1.363 (2)
C4–C5	1.367 (2)	C23–C32	1.484 (2)
C4–H4	0.966 (17)	C24–C25	1.402 (2)
C5–O5	1.3265 (15)	C24–H24	0.938 (17)
O5–H5	1.00 (2)	C25–O25	1.2640 (16)
C6–C7	1.386 (2)	C26–C31	1.3848 (19)
C6–C11	1.3870 (19)	C26–C27	1.392 (2)
C7–C8	1.382 (2)	C27–C28	1.379 (2)
C7–H7	0.9300	C27–H27	0.9300
C8–C9	1.374 (3)	C28–C29	1.376 (3)
C8–H8	0.9300	C28–H28	0.9300
C9–C10	1.378 (3)	C29–C30	1.367 (3)
C9–H9	0.9300	C29–H29	0.9300
C10–C11	1.381 (2)	C30–C31	1.388 (2)
C10–H10	0.9300	C30–H30	0.9300
C11–H11	0.9300	C31–H31	0.9300
C12–H12A	0.9600	C32–H32A	0.9600
C12–H12B	0.9600	C32–H32B	0.9600
C12–H12C	0.9600	C32–H32C	0.9600

Table A4. Continued

Angle	Angle value, °	Angle	Angle value, °
C5–N1–N2	110.46 (10)	C25–N21–C26	129.87 (10)
C5–N1–C6	129.57 (10)	N22–N21–C26	120.54 (10)
N2–N1–C6	119.97 (9)	C23–N22–N21	108.14 (11)
C3–N2–N1	105.48 (10)	C23–N22–H22	123.9 (11)
N2–C3–C4	111.05 (12)	N21–N22–H22	121.0 (11)
N2–C3–C12	120.26 (12)	N22–C23–C24	109.21 (13)
C4–C3–C12	128.67 (13)	N22–C23–C32	119.58 (13)
C5–C4–C3	105.80 (11)	C24–C23–C32	131.20 (14)
C5–C4–H4	127.9 (10)	C23–C24–C25	108.13 (12)
C3–C4–H4	126.3 (10)	C23–C24–H24	125.5 (10)
O5–C5–N1	119.74 (11)	C25–C24–H24	126.3 (10)
O5–C5–C4	133.05 (11)	O25–C25–N21	121.75 (13)
N1–C5–C4	107.21 (10)	O25–C25–C24	132.31 (12)
C5–O5–H5	107.6 (11)	N21–C25–C24	105.94 (11)
C7–C6–C11	120.33 (13)	C31–C26–C27	119.65 (14)
C7–C6–N1	120.64 (12)	C31–C26–N21	120.13 (13)
C11–C6–N1	119.01 (12)	C27–C26–N21	120.21 (12)
C8–C7–C6	119.05 (16)	C28–C27–C26	119.71 (15)
C8–C7–H7	120.5	C28–C27–H27	120.1
C6–C7–H7	120.5	C26–C27–H27	120.1
C9–C8–C7	121.06 (17)	C29–C28–C27	120.69 (17)
C9–C8–H8	119.5	C29–C28–H28	119.7
C7–C8–H8	119.5	C27–C28–H28	119.7
C8–C9–C10	119.44 (15)	C30–C29–C28	119.59 (16)
C8–C9–H9	120.3	C30–C29–H29	120.2
C10–C9–H9	120.3	C28–C29–H29	120.2
C9–C10–C11	120.72 (18)	C29–C30–C31	120.95 (17)
C9–C10–H10	119.6	C29–C30–H30	119.5
C11–C10–H10	119.6	C31–C30–H30	119.5
C10–C11–C6	119.37 (16)	C26–C31–C30	119.39 (16)
C10–C11–H11	120.3	C26–C31–H31	120.3
C6–C11–H11	120.3	C30–C31–H31	120.3
C3–C12–H12A	109.5	C23–C32–H32A	109.5
C3–C12–H12B	109.5	C23–C32–H32B	109.5
H12A–C12–H12B	109.5	H32A–C32–H32B	109.5

Table A4. Continued

C3–C12–H12C	109.5	C23–C32–H32C	109.5
H12A–C12–H12C	109.5	H32A–C32–H32C	109.5
H12B–C12–H12C	109.5	H32B–C32–H32C	109.5
C25–N21–N22	108.38 (11)	–	–
Torsion angle	**Angle value, º**	**Torsion angle**	**Angle value, º**
C5–N1–N2–C3	−0.26 (15)	C25–N21–N22–C23	4.61 (15)
C6–N1–N2–C3	−179.50 (12)	C26–N21–N22–C23	173.22 (12)
N1–N2–C3–C4	0.60 (16)	N21–N22–C23–C24	−4.54 (16)
N1–N2–C3–C12	−178.10 (14)	N21–N22–C23–C32	176.90 (14)
N2–C3–C4–C5	−0.72 (18)	N22–C23–C24–C25	2.76 (17)
C12–C3–C4–C5	177.84 (16)	C32–C23–C24–C25	−178.91 (16)
N2–N1–C5–O5	179.90 (11)	N22–N21–C25–O25	175.97 (13)
C6–N1–C5–O5	−0.9 (2)	C26–N21–C25–O25	8.8 (2)
N2–N1–C5–C4	−0.18 (15)	N22–N21–C25–C24	−2.85 (15)
C6–N1–C5–C4	178.97 (13)	C26–N21–C25–C24	−170.05 (13)
C3–C4–C5–O5	−179.57 (15)	C23–C24–C25–O25	−178.53 (16)
C3–C4–C5–N1	0.52 (16)	C23–C24–C25–N21	0.12 (16)
C5–N1–C6–C7	35.6 (2)	C25–N21–C26–C31	150.33 (14)
N2–N1–C6–C7	−145.28 (12)	N22–N21–C26–C31	−15.54 (18)
C5–N1–C6–C11	−145.78 (14)	C25–N21–C26–C27	−30.3 (2)
N2–N1–C6–C11	33.30 (17)	N22–N21–C26–C27	163.82 (12)
C11–C6–C7–C8	−0.5 (2)	C31–C26–C27–C28	−0.3 (2)
N1–C6–C7–C8	178.05 (12)	N21–C26–C27–C28	−179.65 (13)
C6–C7–C8–C9	−1.2 (2)	C26–C27–C28–C29	1.3 (2)
C7–C8–C9–C10	1.8 (3)	C27–C28–C29–C30	−1.1 (3)
C8–C9–C10–C11	−0.7 (3)	C28–C29–C30–C31	−0.3 (3)
C9–C10–C11–C6	−1.0 (2)	C27–C26–C31–C30	−1.0 (2)
C7–C6–C11–C10	1.6 (2)	N21–C26–C31–C30	178.35 (13)
N1–C6–C11–C10	−176.98 (13)	C29–C30–C31–C26	1.3 (3)

Hydrogen-bond geometry (Å, º)

D–H---A	D–H	H---A	D---A	D–H---A
O5–H5---O25	1.00 (2)	1.49 (2)	2.4794 (14)	169.8 (18)
N22–H22---N2^{i}	0.92 (2)	1.89 (2)	2.8004 (17)	170.5 (16)

Symmetry code: (i) x, $y + 1$, z.

Table A5. Fractional atomic coordinates and isotropic or equivalent isotropic displacement parameters (Å^2) for compound **II**

Atom	*x*	*y*	*z*	U_{iso}*/U_{eq}
Cl1	0.03028 (10)	0.54630 (7)	0.35235 (4)	0.0752 (3)
N1	−0.0218 (2)	0.11695 (18)	−0.17303 (11)	0.0448 (3)
N2	−0.2362 (2)	0.00890 (18)	−0.23953 (12)	0.0491 (3)
H2	−0.3709	0.0045	−0.2140	0.059*
C3	−0.1961 (3)	−0.0883 (2)	−0.35162 (15)	0.0510 (4)
C4	0.0361 (3)	−0.0560 (2)	−0.35717 (15)	0.0510 (4)
H4	0.1068	−0.1099	−0.4241	0.061*
C5	0.1557 (2)	0.0752 (2)	−0.24282 (14)	0.0487 (4)
O5	0.36892 (19)	0.14357 (19)	−0.20424 (12)	0.0616 (4)
C12	−0.3968 (3)	−0.2094 (3)	−0.44703 (18)	0.0706 (5)
H12A	−0.5131	−0.2709	−0.4079	0.106*
H12B	−0.3411	−0.3009	−0.5067	0.106*
H12C	−0.4657	−0.1344	−0.4881	0.106*
C6	−0.0052 (2)	0.21556 (19)	−0.04676 (13)	0.0431 (3)
C7	0.1996 (3)	0.3438 (2)	0.01551 (16)	0.0532 (4)
H7	0.3290	0.3629	−0.0256	0.064*
C8	0.2129 (3)	0.4441 (3)	0.13892 (17)	0.0579 (4)
H8	0.3511	0.5290	0.1816	0.070*
C9	0.0174 (3)	0.4155 (2)	0.19710 (15)	0.0544 (4)
C10	−0.1861 (3)	0.2891 (3)	0.13769 (15)	0.0565 (4)
H10	−0.3152	0.2717	0.1793	0.068*
C11	−0.1989 (3)	0.1865 (2)	0.01432 (14)	0.0520 (4)
H11	−0.3361	0.0990	−0.0270	0.062*

Note: The sign * indicates the isotropic displacement parameters, Å^2.

Table A6. Atomic displacement parameters (Å^2) for compound **II**

Atom	U^{11}	U^{22}	U^{33}	U^{12}	U^{13}	U^{23}
Cl1	0.0948 (5)	0.0763 (4)	0.0413 (3)	0.0189 (3)	0.0047 (3)	−0.0013 (2)
N1	0.0331 (6)	0.0553 (7)	0.0374 (6)	0.0073 (5)	0.0003 (5)	0.0038 (5)
N2	0.0356 (6)	0.0574 (7)	0.0438 (7)	0.0084 (5)	−0.0002 (5)	0.0019 (6)
C3	0.0473 (8)	0.0519 (8)	0.0433 (8)	0.0116 (6)	−0.0036 (6)	0.0002 (6)
C4	0.0460 (8)	0.0585 (8)	0.0416 (8)	0.0166 (6)	0.0047 (6)	0.0015 (6)
C5	0.0395 (7)	0.0617 (8)	0.0426 (8)	0.0147 (6)	0.0049 (6)	0.0104 (7)

Table A6. Continued

Atom	U^{11}	U^{22}	U^{33}	U^{12}	U^{13}	U^{23}
O5	0.0345 (5)	0.0772 (8)	0.0577 (7)	0.0102 (5)	0.0046 (5)	−0.0020 (6)
C12	0.0497 (9)	0.0786 (11)	0.0591 (11)	0.0118 (9)	−0.0054 (8)	−0.0125 (9)
C6	0.0418 (8)	0.0480 (7)	0.0350 (7)	0.0106 (6)	−0.0007 (5)	0.0072 (6)
C7	0.0411 (7)	0.0565 (8)	0.0490 (8)	0.0044 (6)	0.0035 (6)	0.0010 (7)
C8	0.0499 (9)	0.0589 (9)	0.0505 (9)	0.0031 (7)	−0.0035 (7)	0.0028 (7)
C9	0.0633 (10)	0.0550 (8)	0.0410 (8)	0.0165 (7)	−0.0005 (7)	0.0085 (7)
C10	0.0531 (9)	0.0723 (10)	0.0408 (8)	0.0107 (7)	0.0099 (6)	0.0137 (7)
C11	0.0432 (8)	0.0629 (9)	0.0401 (8)	0.0023 (6)	0.0006 (6)	0.0084 (7)

Table A7. Geometric parameters (Å, º) for compound **II**

Atom–Atom	Bond length, Å	Atom–Atom	Bond length, Å
Cl1–C9	1.7562 (18)	C12–H12B	0.9600
N1–N2	1.3843 (17)	C12–H12C	0.9600
N1–C5	1.3914 (17)	C6–C7	1.382 (2)
N1–C6	1.4077 (18)	C6–C11	1.389 (2)
N2–C3	1.349 (2)	C7–C8	1.385 (2)
N2–H2	0.8600	C7–H7	0.9300
C3–C4	1.343 (2)	C8–C9	1.377 (2)
C3–C12	1.488 (2)	C8–H8	0.9300
C4–C5	1.426 (2)	C9–C10	1.364 (3)
C4–H4	0.9300	C10–C11	1.391 (2)
C5–O5	1.2440 (19)	C10–H10	0.9300
C12–H12A	0.9600	C11—H11	0.9300
Angle	**Angle value, º**	**Angle**	**Angle value, º**
N2–N1–C5	108.65 (12)	H12B–C12–H12C	109.5
N2–N1–C6	120.36 (12)	C7–C6–C11	120.05 (14)
C5–N1–C6	129.59 (12)	C7–C6–N1	120.55 (13)
C3–N2–N1	107.82 (12)	C11–C6–N1	119.38 (13)
C3–N2–H2	126.1	C6–C7–C8	120.31 (15)
N1–N2–H2	126.1	C6–C7–H7	119.8
C4–C3–N2	110.05 (15)	C8–C7–H7	119.8
C4–C3–C12	129.74 (16)	C9–C8–C7	118.70 (16)
N2–C3–C12	120.20 (15)	C9–C8–H8	120.6

Table A7. Continued

C3–C4–C5	108.29 (14)	C7–C8–H8	120.6
C3–C4–H4	125.9	C10–C9–C8	122.01 (16)
C5–C4–H4	125.9	C10–C9–Cl1	118.99 (14)
O5–C5–N1	123.33 (14)	C8–C9–Cl1	119.01 (14)
O5–C5–C4	131.64 (14)	C9–C10–C11	119.41 (15)
N1–C5–C4	105.03 (12)	C9–C10–H10	120.3
C3–C12–H12A	109.5	C11–C10–H10	120.3
C3–C12–H12B	109.5	C6–C11–C10	119.51 (15)
H12A–C12–H12B	109.5	C6–C11–H11	120.2
C3–C12–H12C	109.5	C10–C11–H11	120.2
H12A–C12–H12C	109.5	–	–
Torsion angle	**Angle value, º**	**Torsion angle**	**Angle value, º**
C5–N1–N2–C3	−4.19 (17)	C5–N1–C6–C7	24.4 (2)
C6–N1–N2–C3	−171.92 (12)	N2–N1–C6–C11	7.6 (2)
N1–N2–C3–C4	3.76 (19)	C5–N1–C6–C11	−157.28 (15)
N1–N2–C3–C12	−176.41 (16)	C11–C6–C7–C8	0.0 (3)
N2–C3–C4–C5	−1.88 (19)	N1–C6–C7–C8	178.29 (13)
C12–C3–C4–C5	178.31 (19)	C6–C7–C8–C9	−1.1 (3)
N2–N1–C5–O5	−176.12 (15)	C7–C8–C9–C10	1.4 (3)
C6–N1–C5–O5	−9.9 (3)	C7–C8–C9–Cl1	−178.39 (12)
N2–N1–C5–C4	2.98 (16)	C8–C9–C10–C11	−0.6 (3)
C6–N1–C5–C4	169.22 (14)	Cl1–C9–C10–C11	179.25 (12)
C3–C4–C5–O5	178.28 (18)	C7–C6–C11–C10	0.9 (2)
C3–C4–C5–N1	−0.72 (17)	N1–C6–C11–C10	−177.44 (14)
N2–N1–C6–C7	−170.78 (13)	C9–C10–C11–C6	−0.6 (3)

Hydrogen-bond geometry (Å, º)

D–H---A	D–H	H---A	D---A	D–H---A
N2–H2---O5^{i}	0.86	2.02	2.7293 (18)	139

Symmetry code: (i) *x*–1, *y*, *z*.

Table A8. Fractional atomic coordinates and isotropic or equivalent isotropic displacement parameters (Å^2) for compound **III**

Atom	*x*	*y*	*z*	U_{iso}*/U_{eq}
N1	0.48507 (6)	0.37211 (12)	0.10131 (6)	0.0388 (2)
N2	0.47599 (6)	0.54096 (11)	0.13277 (6)	0.0393 (2)

Table A8. Continued

Atom	*x*	*y*	*z*	U_{iso}*/U_{eq}
C3	0.38667 (7)	0.58089 (15)	0.09304 (7)	0.0399 (2)
C4	0.33980 (7)	0.43974 (16)	0.04683 (7)	0.0432 (3)
H4	0.2783	0.4342	0.0164	0.052*
O4	0.38798 (6)	0.14436 (13)	0.02542 (6)	0.0562 (3)
C5	0.40039 (7)	0.29940 (16)	0.05233 (7)	0.0397 (2)
C6	0.56111 (6)	0.26616 (14)	0.15091 (7)	0.0357 (2)
C7	0.59414 (8)	0.14975 (16)	0.11065 (8)	0.0445 (3)
H7	0.5680	0.1449	0.0520	0.053*
C8	0.66604 (8)	0.04131 (17)	0.15833 (9)	0.0490 (3)
H8	0.6882	−0.0366	0.1315	0.059*
C9	0.70529 (8)	0.04735 (17)	0.24529 (8)	0.0475 (3)
H9	0.7532	−0.0271	0.2769	0.057*
C10	0.67305 (8)	0.16467 (17)	0.28522 (8)	0.0451 (3)
H10	0.6998	0.1699	0.3439	0.054*
C11	0.60106 (7)	0.27459 (16)	0.23843 (7)	0.0403 (2)
H11	0.5796	0.3536	0.2655	0.048*
C12	0.35505 (11)	0.75872 (19)	0.10678 (10)	0.0607 (4)
H12A	0.3672	0.8489	0.0747	0.091*
H12B	0.3853	0.7889	0.1657	0.091*
H12C	0.2923	0.7533	0.0888	0.091*
C13	0.54237 (9)	0.67445 (18)	0.14061 (10)	0.0563 (3)
H13A	0.5435	0.6874	0.0874	0.085*
H13B	0.5997	0.6361	0.1827	0.085*
H13C	0.5277	0.7879	0.1569	0.085*

Note: The sign * indicates the isotropic displacement parameters, Å^2.

Table A9. Atomic displacement parameters (Å^2) for compound **III**

Atom	U^{11}	U^{22}	U^{33}	U^{12}	U^{13}	U^{23}
N1	0.0333 (4)	0.0354 (4)	0.0417 (4)	−0.0002 (3)	0.0118 (3)	−0.0046 (3)
N2	0.0368 (4)	0.0299 (4)	0.0447 (5)	−0.0007 (3)	0.0129 (4)	−0.0017 (3)
C3	0.0398 (5)	0.0369 (5)	0.0389 (5)	0.0063 (4)	0.0142 (4)	0.0074 (4)
C4	0.0340 (5)	0.0439 (6)	0.0433 (5)	0.0023 (4)	0.0102 (4)	0.0036 (4)
O4	0.0471 (5)	0.0474 (5)	0.0614 (5)	−0.0062 (4)	0.0135 (4)	−0.0189 (4)
C5	0.0352 (5)	0.0420 (5)	0.0360 (5)	−0.0028 (4)	0.0109 (4)	−0.0027 (4)

Table A9. Continued

Atom	U^{11}	U^{22}	U^{33}	U^{12}	U^{13}	U^{23}
C6	0.0303 (4)	0.0341 (4)	0.0421 (5)	−0.0017 (3)	0.0159 (4)	−0.0018 (4)
C7	0.0435 (6)	0.0450 (6)	0.0456 (6)	0.0011 (5)	0.0209 (5)	−0.0071 (5)
C8	0.0429 (6)	0.0436 (6)	0.0635 (7)	0.0030 (5)	0.0268 (5)	−0.0089 (5)
C9	0.0347 (5)	0.0413 (6)	0.0628 (7)	0.0033 (4)	0.0190 (5)	0.0029 (5)
C10	0.0384 (5)	0.0489 (6)	0.0437 (5)	0.0019 (5)	0.0148 (4)	0.0031 (5)
C11	0.0364 (5)	0.0442 (5)	0.0415 (5)	0.0019 (4)	0.0186 (4)	−0.0027 (4)
C12	0.0625 (8)	0.0443 (7)	0.0662 (8)	0.0174 (6)	0.0212 (7)	0.0044 (6)
C13	0.0495 (7)	0.0408 (6)	0.0707 (8)	−0.0107 (5)	0.0202 (6)	0.0001 (6)

Table A10. Geometric parameters (Å, º) for compound **III**

Atom–Atom	Bond length, Å	Atom–Atom	Bond length, Å
N1–C5	1.4021 (16)	C8–C9	1.379 (2)
N1–N2	1.4098 (13)	C8–H8	0.9300
N1–C6	1.4210 (16)	C9–C10	1.3823 (18)
N2–C3	1.3770 (17)	C9–H9	0.9300
N2–C13	1.4554 (16)	C10–C11	1.3854 (18)
C3–C4	1.3457 (17)	C10–H10	0.9300
C3–C12	1.4860 (18)	C11–H11	0.9300
C4–C5	1.4329 (17)	C12–H12A	0.9600
C4–H4	0.9300	C12–H12B	0.9600
O4–C5	1.2281 (15)	C12–H12C	0.9600
C6–C11	1.3883 (17)	C13–H13A	0.9600
C6–C7	1.3904 (15)	C13–H13B	0.9600
C6–C7	1.3904 (15)	C13–H13B	0.9600
C7–H7	0.9300	–	–
Angle	**Angle value, º**	**Angle**	**Angle value, º**
C5–N1–N2	108.98 (9)	C7–C8–H8	119.6
C5–N1–C6	123.53 (10)	C8–C9–C10	119.68 (11)
N2–N1–C6	118.50 (9)	C8–C9–H9	120.2
C3–N2–N1	106.22 (9)	C10–C9–H9	120.2
C3–N2–C13	121.31 (10)	C9–C10–C11	120.42 (12)
N1–N2–C13	115.25 (10)	C9–C10–H10	119.8
C4–C3–N2	110.46 (11)	C11–C10–H10	119.8

Table A10. Continued

C4–C3–C12	129.58 (12)	C10–C11–C6	119.61 (11)
N2–C3–C12	119.94 (11)	C10–C11–H11	120.2
C3–C4–C5	108.73 (11)	C6–C11–H11	120.2
C3–C4–H4	125.6	C3–C12–H12A	109.5
C5–C4–H4	125.6	C3–C12–H12B	109.5
O4–C5–N1	123.29 (11)	H12A–C12–H12B	109.5
O4–C5–C4	131.71 (11)	C3–C12–H12C	109.5
N1–C5–C4	104.94 (10)	H12A–C12–H12C	109.5
C11–C6–C7	120.02 (10)	H12B–C12–H12C	109.5
C11–C6–N1	120.88 (10)	N2–C13–H13A	109.5
C7–C6–N1	119.08 (10)	N2–C13–H13B	109.5
C8–C7–C6	119.56 (12)	H13A–C13–H13B	109.5
C8–C7–H7	120.2	N2–C13–H13C	109.5
C6–C7–H7	120.2	H13A–C13–H13C	109.5
C9–C8–C7	120.70 (11)	H13B–C13–H13C	109.5
C9–C8–H8	119.6	–	–
Torsion angle	**Angle value, º**	**Torsion angle**	**Angle value, º**
C5–N1–N2–C3	−8.50 (11)	C3–C4–C5–O4	174.74 (13)
C6–N1–N2–C3	−156.86 (9)	C3–C4–C5–N1	−2.69 (13)
C5–N1–N2–C13	−145.85 (11)	C5–N1–C6–C11	−112.19 (12)
C6–N1–N2–C13	65.80 (14)	N2–N1–C6–C11	31.29 (14)
N1–N2–C3–C4	6.83 (12)	C5–N1–C6–C7	66.27 (14)
C13–N2–C3–C4	141.00 (12)	N2–N1–C6–C7	−150.25 (10)
N1–N2–C3–C12	−174.78 (10)	C11–C6–C7–C8	0.83 (17)
C13–N2–C3–C12	−40.61 (17)	N1–C6–C7–C8	−177.64 (11)
N2–C3–C4–C5	−2.62 (13)	C6–C7–C8–C9	0.02 (18)
C12–C3–C4–C5	179.20 (12)	C7–C8–C9–C10	−0.78 (19)
N2–N1–C5–O4	−170.83 (11)	C8–C9–C10–C11	0.70 (18)
C6–N1–C5–O4	−24.42 (17)	C9–C10–C11–C6	0.15 (18)
N2–N1–C5–C4	6.87 (11)	C7–C6–C11–C10	−0.91 (17)
C6–N1–C5–C4	153.29 (10)	N1–C6–C11–C10	177.53 (10)